

Water supply to a geotechnical centrifuge for pile jetting in sand

P. Shepley

University of Sheffield

M.D. Bolton

University of Cambridge

ABSTRACT: The supply of water is often required during a centrifuge experiment. For the case of pile jetting; significant flow volumes and pressures are required from the water supply. This paper aims to detail the successful provision of water at high pressures and large flow rates to a centrifuge, using a novel water supply system. An impeller pump was used to pressurise the water in advance of the slip rings, with further pressure provided by the fluid accelerating along the centrifuge beam arm. A maximum pressure of 2 MPa and continuous flow rate of 6 litres per minute were achieved. The calculation of water pressure away from the measurement location is presented, offering a repeatable solution for the pressure at any point in the pipe work.

1 INTRODUCTION

1.1 *Jacked piling*

Jacked, or silent, piling is an increasingly common method for pile installation. Low impact means of installing piles are desirable for construction projects in urban or sensitive areas. Jacked piling is often selected for this purpose due to its production of little noise and few ground vibrations (White et al. 2000).

However, jacked piles are restricted by the maximum deliverable installation force. For counterweight systems, this is limited by the amount of available kentledge. In the case of the piler system produced by Giken Seisakusho Ltd., a Japanese piling contractor, reaction force is provided by the previously installed piles in the pile wall. Both techniques are fundamentally load limited. If the piling load approaches the maximum available load, the installation rate may fall to an uneconomical rate or even pile refusal in the most extreme cases.

A supplementary technique can be used to reduce the required installation loads. The aim of any such technique is to maintain the advantages of the installation, with low noise and vibration, but also reduce the installation load such that jacking can still be achieved at an economical rate. Alternative techniques exist to achieve this, such as surging, pre-augering and gyropiling. The use of supplementary water jetting during pile installation is of particular interest for this study. Jetting was chosen for its ease of implementation, retaining the strengths of jacked piling whilst reducing the maximum required installation loads.

1.2 *Water jetting*

Water jetting has been in use for decades, mainly for offshore applications (Tsinker 1988). The offshore environment provides a large readily available water source and an open area with no nearby structures that may be affected by the use of water jetting. Typical flow rates for the process exceed 1500 litres per minute in all soil types.

Tsinker's mechanism relies on fluidizing the ground around the pile location. This allows the pile to install under self weight. In order to key the pile toe into undisturbed soil at the end of installation, Tsinker suggests hammering the pile for a further 0.5 m to ensure reasonable final pile strength. This requirement highlights the destructive nature of the jetting mechanism.

The technique has since improved to allow its more widespread use. Lower flow rates are specified. However, the suggested peak flow rate is 1000 litres per minute (Tomlinson and Woodward 2008).

Furthermore, water jetting can be used in conjunction with another, established, piling method. This further reduces the required flow rate during the jetting process. Combining water jetting with pile jacking, bulk fluidization of the ground around the pile, like Tsinker, is no longer required to install the pile. Instead, smaller flow rates are used to soften the ground and allow faster pile jacking to take place in hard ground conditions. For this process, the required flow rate can fall below 600 litres per minute in all soil conditions; providing flow can be maintained for the entire installation depth. Pump

pressures greater than 2 MPa are also observed during the jetting process.

However, there have been few studies completed on combined water jetting with pile jacking. The reduction of installation load has been broadly established from field testing, but the governing mechanism is still unknown. Different analyses have been suggested, most recently the scour system outlined by Schneider et al. (2008), yet further research is required to fully investigate the mechanism.

In order to investigate the mechanism in more detail, further centrifuge modelling of water jetting was completed at University of Cambridge using the 10 m diameter Turner Beam Centrifuge. A novel system for the provision of water to the experiment was designed to achieve modelling similitude of water jetting in sand.

2 CENTRIFUGE MODELLING

2.1 Previous studies

Centrifuge modelling of water injection systems has previously been completed. A study by Schneider et al. (2008) was conducted into the effect of water jetting with pile jacking. Water flow was derived using a displacement controlled syringe pump, where a fluid filled piston was driven using a linear actuator. During testing, a maximum pressure of 25 kPa was achieved at the pile head and low flow rates of 0.15-0.22 litres per minute sustained through the pile.

These injection properties are much lower than experienced in the field, where pressures exceed 2 MPa and flow rates reach 600 litres per minute.

The jetting parameters of Schneider were sufficient to generate a significant jetting effect in silt: whereas the effect in sand was negligible. This is due to the different governing mechanism for water jetting in silts and sands. In silts, a small change in the pore pressure adjacent to the pile can be induced using a small flow rate, and a reduction in installation load observed. Whereas in sand, a larger flow rate is required in order to observe similar changes in the installation load.

Therefore, larger flow rates and increased pressures are required to achieve a notable effect from jetting in sands. These are required in order to achieve similitude of water pressure between the model and prototype scale. In order to achieve this, a different water provision system, specified in the next section, is required.

2.2 Design of a novel water supply system

The new system was designed to deliver pressures greater than 2 MPa, to match the pressure at prototype scale, and to sustain high flow rates for the duration of pile installation, 160 seconds in this case.

This was not possible using a similar displacement controlled syringe pump mounted on the centrifuge experiment package.

To achieve the required high pressures, water would be supplied to the package through the hydraulic slip rings and down the centrifuge arm. From a combination of pressurizing the fluid upstream of the slip rings and the radial acceleration down the beam arm, maximum pressures exceeding 2 MPa at the package could be consistently achieved.

The contribution from the acceleration down the beam can be calculated using:

$$P_{package} = P_{slip\ rings} + 0.5 \rho \omega^2 (r_{package}^2 - r_{slip\ ring}^2) \quad (1)$$

where P is the pressure at the package and slip rings measured in Pascal, ω the angular velocity of the centrifuge in radians per second, and r the radius from the centre of the beam of the package and slip rings in metres.

The water pressure and flow rate were monitored at the package, upstream of the pile, using the 'high pressure line' shown in Figure 1. A pulsing flow meter was used to determine the flow rate and a 3.5 MPa pressure transducer used to monitor the pressure at this location in the water supply.

Water was supplied to the slip rings using a small impeller pump. This could supply 7 litres per minute at pressures up to 700 kPa. The pressure and flow rate were monitored between the pump and the slip rings. In addition, a servo controlled orifice valve was also placed between the pump and the slip rings, in order to control the flow being supplied to the pile. Figure 2 shows the apparatus used at the pump.

Combined, this system delivered peak pressures of 2 MPa at the high pressure line at 60g acceleration.

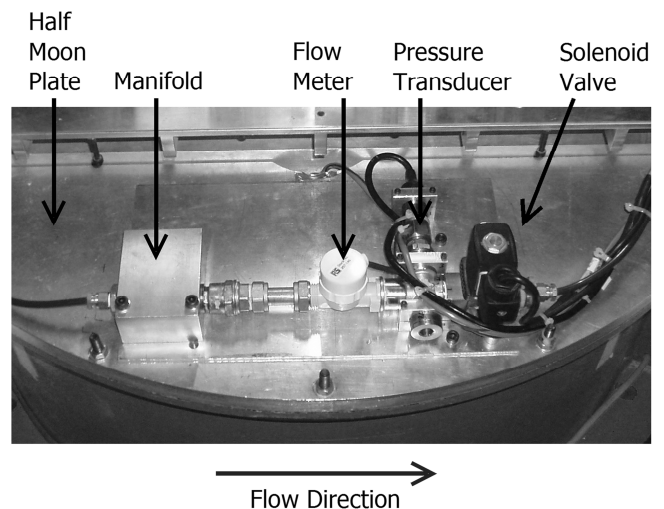
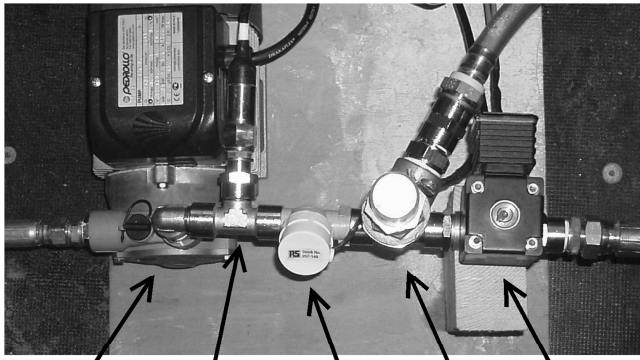


Figure 1. Photograph of the high pressure line on the centrifuge package. The flow meter and pressure transducer are used to monitor the flow. The solenoid valve triggers the flow. The pile toe is 1.5 m downstream of the high pressure line



Impeller Pump Pressure Transducer Flow Meter Relief Valve Control Valve

Figure 2. Photograph of the pump system and associated apparatus. The flow meter and pressure transducer provide additional information on the flow condition at this point. The control valve can be remotely operated to change the flow rate provided to the centrifuge.

2.3 Pressure calculations

The water conditions were measured far from the pile toe. This was to simplify the positioning of the instrumentation. However, it was important to find the water pressure at the pile toe in order to investigate the various soil responses to the use of supplementary water jetting for pile installation.

The pressure at the pile toe was calculated using an adapted Bernoulli's equation (Goforth et al. 1991). Equation 2 allows the pressure at the pile toe, point 2, to be found based on the monitored conditions at the high pressure line, point 1. The energy loss from the flow between the two locations is represented by ΔE .

$$P_1 + \frac{V_1^2 \rho}{2} - \frac{\omega^2 r_1^2 \rho}{2} = P_2 + \frac{V_2^2 \rho}{2} - \frac{\omega^2 r_2^2 \rho}{2} + \Delta E \quad (2)$$

where V is the flow velocity in metres per second, and ρ the fluid density in kilograms per metre cubed.

The energy loss between the high pressure line and the pile toe had to be determined for each nozzle used during testing. This is presented in more detail in Section 3.

2.4 Model construction

A fine sand body was prepared to 80 % relative density in a centrifuge container, 850 mm in diameter. The model depth was 320 mm. The sand model was saturated from the base with de-aired water.

A unique fine sand was prepared for the course of testing. Fraction E silica sand was mixed with commercially available kiln dried builders sand. To ensure consistency between the different models, the sand was repeatedly sampled and the particle size distribution of the sand determined using the single particle optical sizing technique (White 2002).

Table 1. Properties of mixed fraction of sand

Sand	Mixed fraction
d_{10} (mm)	0.192
d_{60} (mm)	0.525
C_c	1.120
C_u	2.734
e_{min}	0.488
e_{max}	0.862
ϕ_{crit}	34.6
k (mm/s)	0.10

The sand properties are listed in Table 1.

2.5 Model pile

A bespoke instrumented model pile was constructed for the testing program. A stainless steel tube of 12 mm outside diameter was used, with a water delivery pipe running through the centre. Stainless steel was selected for its strength, hardness and resistance to corrosion: preventing buckling during testing and any significant surface abrasion from multiple installations. This ensured consistency over all installations during testing. A photograph of the pile is shown in Figure 3.

Strain gauges were used to monitor the axial load at the pile toe and pile head. Two full Wheatstone bridges were used at each location.

The water delivery pipe was a 2.5 mm internal diameter plastic pipe. This terminated at a detachable nozzle at the pile toe. Different nozzles were used throughout the testing program. The nozzles used were either simple orifice plates or more complex multi-exit nozzles. The orifice nozzles all had central holes, 1.0, 2.5 and 3.0 mm in diameter. The two multi-exit nozzles used four 1.5 mm diameter holes for the flow to exit through. The cone nozzle had four holes on the base of the pile, equally spaced and 2 mm from the outer circumference. The side nozzle again had the four holes equally spaced, but 2 mm above the pile base on the side of the pile.

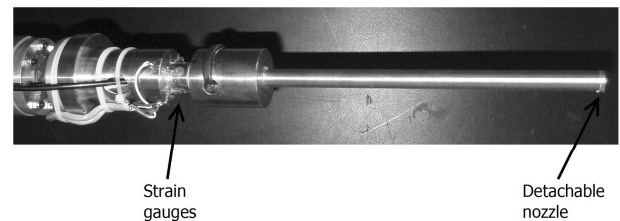


Figure 3. Photograph of the pile used during testing. Strain gauges are attached to the pile at the pile head as marked and at the pile toe, just above the detachable nozzle. A range of nozzles could be attached to the pile over the course of testing.

2.6 Testing program

Any pile installations presented in this paper were completed at a model acceleration of 60g. According to length scaling (Ko 1988), this modelled a 720 mm diameter close ended tubular pile, installed to a depth of 11.4 m. For the purpose of future discussions, all units will be displayed at the model scale.

A soil stabilization loop was completed before the first installation in order to prevent excessive change of the sand body between the first and subsequent flights. Following this, multiple pile installations were completed in a single flight using The Schofield Centre's 2D Actuator (Haigh et al 2010). Piles in a single flight were spaced at 140 mm (12D_p), but the final pile spacing was 70 mm (6D_p).

3 RESULTS

3.1 Flow testing

Flow tests were completed for each nozzle used during testing. This was required to find the energy loss between the high pressure line and the pile toe.

Each test involved passing a constant flow rate through the pile for a period of 20-30 seconds. During the flow test the pile toe was suspended above the sand surface and atmospheric pressure at the pile toe was assumed. Flow tests were completed at 1, 20, 40 and 60g intervals, with a variety of flow rates trailed at each acceleration level by varying the control valve position. The aim of testing was to find a linear relationship between the energy loss in the system and the flow rate squared, satisfying the equation

$$\Delta E = a \times Q^2 \quad (3)$$

To find the energy loss for each data point, the data was assessed using Equation 2. Figure 4 shows the results from the flow testing. Table 2 tabulates the energy loss factor for each nozzle and the R-squared value for the linear regression.

The data points fit well to a straight line through the origin for each nozzle used. The similarity between the 2.5 and 3.0 mm orifice nozzles was expected, due to their similar size to the delivery pipe running through the pile. This would eliminate the difference in exit loss for the two nozzles, giving a good test of consistency within the system.

Table 2. Values of loss coefficients

Nozzle	Loss coefficient, a	R ² value
1.0 mm	18.84x10 ¹⁴	0.967
2.5 mm	1.93 x10 ¹⁴	0.988
3.0 mm	1.99 x10 ¹⁴	0.974
cone	3.34 x10 ¹⁴	0.976
side	2.51 x10 ¹⁴	0.922

3.2 Calculation of pressure at the slip rings

The pressure at the slip rings could also be calculated using Equation 2. The calculation allows the pressure at all key points in the system to be assessed.

The slip ring pressure calculation can be based either on the measurements at the high pressure line or at the pump. However, due to the presence of the lossy control valve, the initial calculation will be based on the high pressure line measurements.

The data from flow testing was used to find the pressure at the slip rings, P_s. The energy loss term was calculated based on standard pipe loss formulae, as used in industry.

The calculations predict large negative pressures arising at the slip rings. The minimum pressure was -400 kPa. This is much lower than the cavitation pressure of water and cannot be sustainable in a fully saturated pipe work system.

To resolve this, the slip ring pressure was found based on data from the pump measurements. Using this data, it is unclear how the large negative pressures are derived. A large pressure drop across the control valve is predicted at low flow rates, due to the small orifice size, but this should not result in such a negative pressure.

To understand the prediction of large negative pressures, the condition at the slip rings needs to be considered. If air can enter this point of the system, due to zero or slightly negative pressure, then the pressure will quickly equalise with the atmospheric pressure. Any air entering the system poses no blockage to the flow, and water would continue to pass through the air gap in the pipe work.

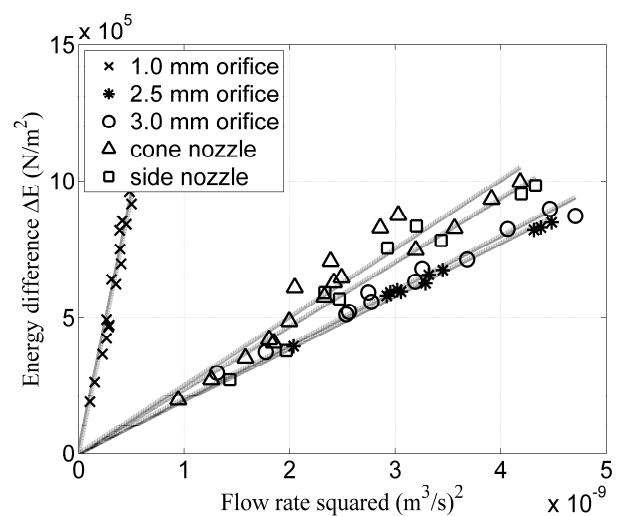


Figure 4. Energy loss per unit volume of fluid passing between the high pressure line and the termination nozzle at the pile toe. Different trends are plotted for the individual nozzles tested during the flow testing. The gradient of the line of best fit gives the loss coefficient for the nozzle, shown in Table 2.

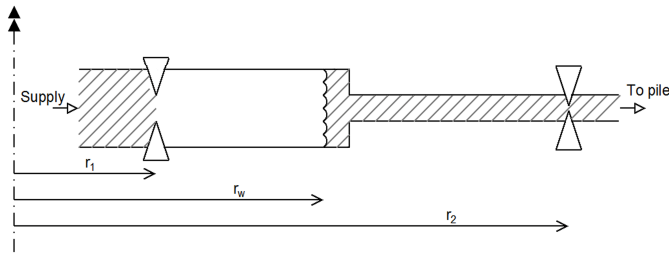


Figure 5. An illustration of the system with the air filled void present between the slip rings, at r_s , and the phreatic water surface, r_w . The water column between r_w and r_2 , at the high pressure line, is ultimately driving the flow through the pile. At steady state, this is equal to the flow rate delivered to the centrifuge through the slip rings.

This assumption of air entry was corroborated during the experiment. Visible bubbles were present in the flow system, which appeared to flow in the opposite direction to the flow during low flow rate periods. This coincided with moments where the input flow to the centrifuge was heavily constrained using the flow control valve.

If air can enter the system via the slip rings, then air can be present throughout the system. This violates the original assumption of a fully saturated system, and instead the system must be assessed as partially saturated.

During a period of low flow rate, less flow is supplied to the centrifuge than the achievable flow rate through the pile. The column of water along the beam arm above the pile generates sufficient pressure without any additional pressure from the slip rings to drive the flow. The column of water drains from the pipe work along the beam arm until equilibrium is reached. At this point, the flow provided to the centrifuge is equal to the flow rate through the pile, caused by the pressure from the column of water along the beam arm alone. An illustration of this is shown in Figure 5.

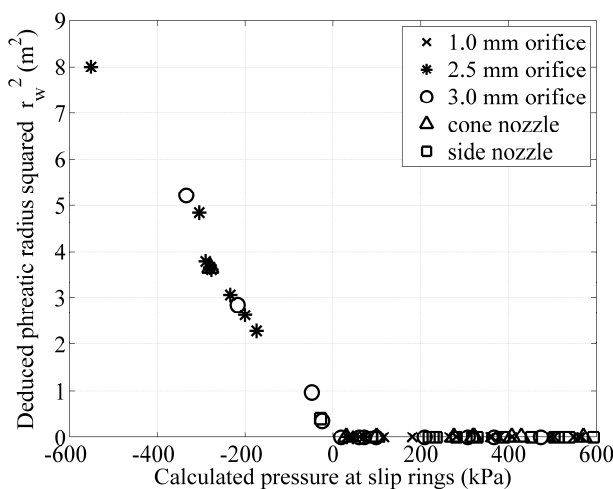


Figure 6. Deduced location of the phreatic surface for the different nozzles and systems tested. The phreatic radius, r_w , always sits between the high pressure line and the limit of the slip rings on the centrifuge.

The figure illustrates how the air filled gap interacts with the water. Water flowing through the valve at a restricted flow rate, accelerates through the air void towards the phreatic water surface at r_w . This marks the top of the saturated water column above the pile that provides pressure to the high pressure line and the pile.

Figure 6 shows the deduced values for the water surface position for the partially saturated system, plotted against the calculated pressure at the slip rings assuming the system is fully saturated. When the slip ring pressure falls negative, the calculation corrects for this and allows an air void to form. The more negative the slip ring pressure, the larger the air void required. As the formation of the air void is controlled by a limitation of the supplied flow rate, it is clear that the flow rate is reducing for the enlarging air void.

To ensure the effect was due to the combination of allowable free flow through the pile and limitation of the flow supply, a similar calculation was repeated for the flow data logged during a pile installation. Throughout the installation, the control valve is held fully open, but the flow through the pile is limited by the nozzle interacting with the soil. The logged data was analysed using the same method as the flow check data, to investigate the pressure at the slip rings. At no point did the pressure fall negative, despite the near zero flow rates sustained through the system. This result confirmed that an air void was induced into the water supply system by constricting the flow supply to the slip rings.

3.3 Calculating the toe pressure

The pressure at the pile toe can be predicted throughout an installation, based on Equation 2. This accounts for the changing position of the toe in the acceleration field and the energy loss as the flow passes from the measurement location to the nozzle termination.

Best practice would be to include a pressure transducer as close as possible to the pile toe, in order to minimize the error in finding the toe pressure. This is not always possible during centrifuge operations, however a consistent analysis system can be operated if the energy loss between the measurement location and the point of interest is well defined.

4 INSTALLATION RESULTS

Multiple centrifuge tests were completed on identical sand bodies. The sand bodies were tested for their continuity via a control installation, without using water jetting. This was effectively a penetration test and gave a reference installation to compare

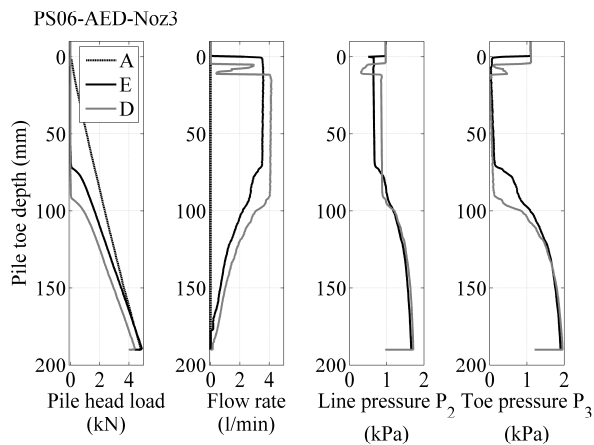


Figure 7. Comparison of the effects of different flow rates. Installation A is the control installation without water jetting. Installations E and D are two installations using jetting.

other installations to, as well as a comparator between different sand bodies used over the multiple test weeks. There was good agreement between the quality of the sand bodies used.

Figure 7 compares the result of different installations. Three installations are shown, one without water injection, A, and two with water injection, D and E. The same 3.0 mm diameter orifice nozzle is used in all three installations, but the flow rate is changed between the two jetted installations.

Using water injection initially reduces the pile load to zero. During this region of zero load, the flow rate sustained to the pile remains as high as possible. Following this initial phase of installation, the flow rate begins to throttle off due to the interaction of soil with the nozzle at the pile base. The flow rate reduction results in a smaller flow energy loss, and a higher nozzle pressure at the pile toe. Yet despite this higher nozzle pressure, the flow rate continues to reduce with increasing depth. The flow rate continues to reduce with increasing depth, until terminating as the pile approaches full depth. Throughout the installations, the flow input parameters remain unchanged, and any change in the flow rate is due to the soil response around the pile installation.

Comparing the two water injection aided installations: the larger flow rate provides a larger toe pressure. This allows the pile to be installed with zero load to a greater depth. Therefore, the higher the toe pressure that can be sustained during installation, the further the pile can be installed without generating any resistance to pile installation. At greater depths, the pile can continue to be installed with lower installation loads due to the sustained higher flow rate and toe pressure.

5 CONCLUSIONS

In conclusion, a novel system was successfully commissioned for the provision of water at high pressures and large flow rates to a centrifuge ex-

periment. The system worked well on the large diameter beam centrifuge at University of Cambridge. Peak pressures of 2 MPa and peak flow rates of 6 litres per minute could be sustained for prolonged periods.

Flow control was implemented using a simple orifice control valve. The valve provided adequate control during pile installations and a wide range of consistent flow rates were achieved. However, care was required when operating at low flow rates, due to the possibility of air entrapment in the system.

An energy approach was used to assess the pressure at locations remote to the available measured data. Of particular interest was finding the pressure at the nozzle, in order to determine the conditions in the soil during the water jetting process. Several flow rate checks were required to accurately assess the energy loss in the pipe work between the point of interest and the measured location. Properly assessed, the energy loss approach offered a repeatable method for finding the nozzle pressure throughout the testing completed. However, it must be accepted that best practice is to monitor the flow conditions as close to the point of interest as possible in order to minimize the uncertainty in the calculations.

Finally, a high quality data set for a range of differently jetted installations was collected. The toe pressure is known throughout these tests, allowing the fundamental mechanism behind water jetting to be more thoroughly understood.

6 ACKNOWLEDGEMENTS

The authors would like to thank Giken Seisakusho Ltd. for their continued support throughout the duration of the research.

7 REFERENCES

- Goforth G., Townsend F. and Bloomquist D. 1991. Saturated and unsaturated fluid flow in a centrifuge. In *Centrifuge '91*, 497-502.
- Ko H.Y. 1988. Summary of the state-of-the-art in centrifuge model testing. In *Centrifuges in Soil Mechanics*, 11-18, Rotterdam.
- Schneider J.A., Lehane B.M. and Gaudin C. 2008. Centrifuge examination of pile jetting in sand. In *2nd IPA workshop*, 17-24 New Orleans.
- Tomlinson M. and Woodward J. 2008. *Pile design and construction*. Taylor & Francis, London
- Tsinker G.P. 1988. Pile jetting. *Journal of geotechnical engineering* 114(3), 326-334.
- White D.J., Sidhu H.K., Finlay, T.C.R., Bolton M.D. and Nagayama T. 2000. The influence of plugging on driveability. In *8th international conference of the deep foundations institute*, 299-310. New York.
- White D.J. 2002. PSD measurement using the single particle optical sizing (SPOS) method. *Géotechnique*, 53(3), 317-326.